Bull. Mater. Sci., Vol. 31, No. 6, November 2008, pp. 907–918. © Indian Academy of Sciences.

Synthesis and characterization of monoclinic rare earth titanates, $RE_2Ti_2O_7$ (RE = La, Pr, Nd), by a modified SHS method using inorganic activator

K KRISHNANKUTTY and K R DAYAS*

Department of Chemistry, University of Calicut, Calicut University P.O., Malappuram District 673 635, India

MS received 18 February 2008; revised 14 May 2008

Abstract. **The nano particles of phase pure rare earth titanates, synthesized by the SHS technique, get well sintered at lower temperatures compared to the compounds formed by the solid-state method. These dielectrics are highly stable and can be used in the microwave frequency range. We report here a modified SHS method to synthesize phase pure monoclinic $RE_2Ti_2O_7$ at 350°C through the oxide/nitrate precursors using an inorganic compound, ammonium acetate, in place of the general type of organic activators such as urea, alanine etc. The nanopowders of $La_2Ti_2O_7$, $Pr_2Ti_2O_7$ and $Nd_2Ti_2O_7$ on heating exhibit an exothermic behaviour with a broad maxima in the range 267–284°C and become endothermic with maxima in the range 1043–1220°C; interestingly, the phase pure crystalline material is formed at the temperature of exothermic maxima, as confirmed by XRD.**

Keywords. **Rare earth titanates; SHS; phase pure $RE_2Ti_2O_7$; inorganic activator; MW dielectrics; nano particles.**

1. Introduction

Several processing techniques (Nadkarni 1991; Buchanan 1993) are available for the commercial production of nano particles of electroceramic materials. Modern synthetic methods like alkoxide process (Chaput *et al* 1990; Katayama *et al* 1996), sol–gel method (Reed 1989), hydrothermal technique, micro emulsion method, vapour phase reactions, etc have limited acceptance by the industry due to the high cost of reactants and the limitations of upscaling the process. Therefore, such compound oxides are still widely produced by the solid-state method in which other impurity phases are likely to be formed during the process, requiring repeated sintering and milling to get phase pure products. Several improvements are attempted at different stages in the solid-state methods, such as pyrolysis of complex compounds like metal oxalates, citrates, catecholates, etc. Certain modifications of the solid-state route to get phase pure functional ceramic materials having desired properties and applications are also reported. Of these, perhaps the most important is the self propagated high temperature synthesis (SHS). Compared to other methods, SHS offers a highly cost effective method for the manufacture of ceramics (Grigorev and Merzhanov 1992; Grigoryan 1997; Matkowsky 1997; Patil *et al* 2002) due to several factors such as (i) utilization of reaction heat generated during the reaction instead of external power, (ii) high combustion temperature and burning velocity, (iii) simplicity of experimental set up and (iv) high quality of the products. In general, SHS is a material and energy saving process (Hwang 2004). Rare earth (RE) titanates are generally prepared by sintering the constituent oxides at high temperatures (Kestigian and Ward 1955) but phase pure materials are seldom obtained. The organic fuels based SHS method also need not yield completely phase pure compounds. But our modified SHS method, using an inorganic activator, ammonium acetate (in place of the traditional organic activators like urea, citric acid, glycine, alanine etc), ensure formation of completely phase pure monoclinic rare earth titanates, $RE_2Ti_2O_7$ (RE = La, Pr, Nd).

The rare earth titanates of La, Pr and Nd have a number of applications. For example, lanthanum titanate, in the pyrochlore structure, $La_2Ti_2O_7$, or in the perovskite modification, $La_{2/3}TiO_3$, conducts photocurrent in the UV region (Kimura *et al* 1972; Scheunmann and Muller 1975; Xiong *et al* 1996), as thin films exhibit optical wave guiding properties (Xiong *et al* 1996; Takeda *et al* 2003). It exhibits piezoelectric properties at very high temperatures (Takeda *et al* 2003) as it has an extraordinary high T_c of 1500°C and can conveniently be used above 1000°C for controlling intelligent gas turbine engines. It sustains very high-applied fields from 0·1 V/cm to 80 kV/cm with-

*Author for correspondence (krdayas@hotmail.com)

out dielectric breakdown. It has been observed that addition of $Nd_2Ti_2O_7$ to yttria doped stabilized zirconia (8Y-FSZ) increased its fracture toughness (Liu and Chen 2005). Multi layer ceramic chip capacitors (MLCCs) containing neodymium titanate enables the use of low cost internal electrode material like 70 Ag/30Pd in place of the expensive Pd or Pt.

Most of these applications are dependent on phase purity, stoichiometry, particle size, surface area and various physico-chemical and structural parameters of the product. We report the advantages of synthesis of electroceramic rare earth titanates, $RE_2Ti_2O_7$ (RE = La, Pr, Nd), by the modified SHS method from RE_2O_3 and TiO_2 using ammonium acetate as the activator over the solid state method and the SHS reaction using urea.

2. Experimental

2.1 *Materials*

The rare earth oxides, La_2O_3, Pr_6O_{11} and Nd_2O_3 of purity > 99% (Indian Rare Earths Limited, Kerala, India) and TiO_2, 99% (Merck India Limited), prior to their use were quantitatively analysed using X-ray fluorescence spectrometer (XRF). The minor impurities contained in these oxide precursors are SiO_2, SO_3, Al_2O_3, CaO, MgO and MnO. The ammonium acetate of 99% purity (Merck India Limited) was used and all other reagents and chemicals used were of analytical grade.

2.2 *Synthesis of rare earth titanates*

For comparison of the process advantages, the rare earth titanates were prepared by the SHS method using urea (organic activator) and ammonium acetate (inorganic activator) and also by the conventional solid state method.

2.2a *Solid-state synthesis*: TiO_2 (0·04 mol) and RE_2O_3 (0·02 mol) were mixed homogenously in presence of isopropanol (15–20 ml) and dried in air. To this, required amount of 5% aqueous solution of poly vinyl alcohol (PVA) of mol. wt. ~ 1,25,000, and purity 98·50%, was added to ensure 1·5% solid PVA in the mix (after drying). The bindered material was dried, and granulated. The granules were compacted at a pressure of 200–300 MPa to discs of 6 mm ∅ and about 1 mm thickness. These discs were sintered at temperatures of 1350°C, 1400°C, 1450°C, 1500°C and 1550°C.

2.2b *SHS using urea as activator*: Rare earth oxides are generally more stable and less reactive compared to their salts such as nitrates, halides, etc hence the oxides were first converted to nitrates prior to the SHS reaction. 0·02 mol of the rare earth oxides were dissolved in hot 1 : 1 HNO_3 and evaporated to dryness on a boiling water bath. To this, 0·04 mol TiO_2 and 0·08 mol urea were added and heated on an electric Bunsen. At a temperature of ~ 350°C copious brown fumes of oxides of nitrogen start evolving. A spontaneous incandescent reaction takes place vigorously with bright flame along with evolution of large amount of gases. The contents froth up to a highly porous network of foam like structure, which almost fills the reaction vessel.

2.2c *SHS using ammonium acetate as the activator*: The rare earth nitrates (0·04 mol) were prepared from RE oxides (RE = La, Pr, and Nd) as described above. To this 0·06 mol ammonium acetate was added and the mixture was dissolved in water (~ 100 ml) to get a clear solution. 0·04 mol of TiO_2 was added to this and vigorously stirred to keep the fine particles of TiO_2 in suspension. The solvent evaporated off on a water bath. The dry reactants were heated on an electric Bunsen. As the temperature reaches ~ 350°C brown fumes start evolving from the mixture and an incandescent reaction sets in with smoke and flame in the vessel with a bright glow. Due to the evolution of large amounts of gases, the mixture froths. At the peak of the reaction, the products (being very light and fine) starts flying fast out of the reaction vessel as 'fireworks flower pots'; the tendency for flying out is accelerated by the liberation of hot gases at this stage. A conical shaped wide collector was placed at the mouth of the reaction vessel to collect the flying off particles.

2.3 *Measurement of dielectric properties*

Silver electrodes were fixed on the surfaces of the sintered discs by applying silver paste and curing at 760°C. Tinned copper wire leads were attached by soldering and then encapsulated using epoxy resin powder. The capacitance and loss factor (tan δ) were measured at frequencies, from 100 Hz to 10 MHz. The permittivity values were calculated. The permittivity values (ε_r) and loss factor were plotted against the corresponding frequencies.

2.4 *Instrumentation*

The oxides of rare earths and TiO_2 were quantitatively analysed using Philips PW 2400 model sequential wavelength dispersive X-ray fluorescence spectrometer (XRF). XRD patterns of the samples were recorded using Bruker AXS 5005 model X-ray diffractometer with CuK_α radiation (λ = 1·5418 Å) with Ni filter at 40 kV and 30 mA. The BET surface area was measured using Quanta chrome Nova model 1200 BET analyser and the average particle size (APS) calculated.

The SEM microstructures were studied using JEOL JSM-840A SEM. Thermal properties were measured using Perkin Elmer Pyris Diamond model TG-DTA. After calcining the SHS powders at different temperatures (600–

Table 1. Thermo chromic property of $RE_2Ti_2O_7$ with sintering temperature.

Sl. no.	$RE_2Ti_2O_7$	Colour before sintering	Colour at sintering temperature		
			1350–1400°C	1400–1500°C	Above 1500°C
1.	$La_2Ti_2O_7$	White	Light rose	Yellow	Golden cream
2.	$Pr_2Ti_2O_7$	Black	Yellow	Green	Dung green
3.	$Nd_2Ti_2O_7$	Light rose	Brown	Brown	Brown

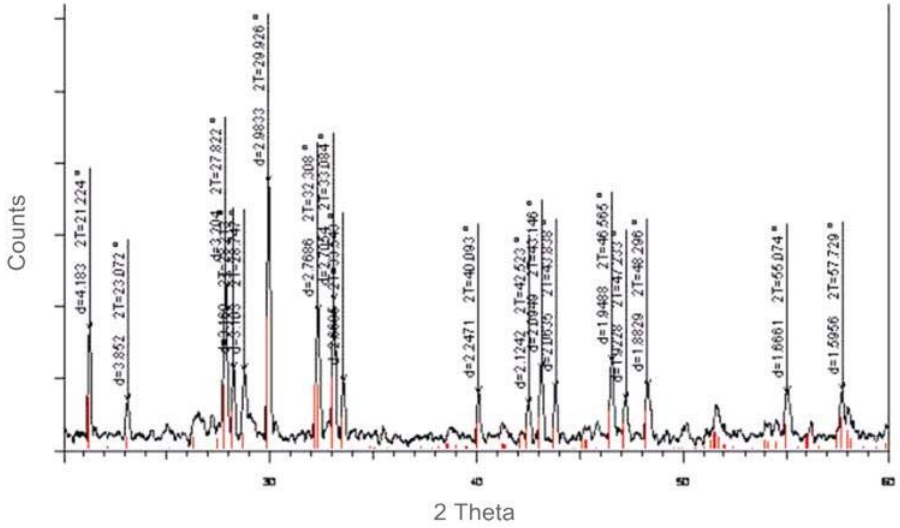

Figure 1. XRD of monoclinic $La_2Ti_2O_7$ synthesized by SHS-urea method and calcined at 1200°C (Match ICDD 28-0517).

1200°C), the XRD patterns were taken. The FT–IR and Raman spectra were taken for the calcined (at 1200°C) SHS powders. The Raman spectra were recorded using Bruker FT-Raman, model IFS-66V/FRA-106 and FTIR spectra using Thermo-Nicolet Avatar 370 or Shimadzu 8400S-CE. The capacitance and loss factor (tan δ) were measured at frequencies, from 100 Hz to 10 MHz using an Agilent Gain phase Analyser HP- 4294 A.

3. Results and discussion

3.1 *Structural characteristics of rare earth titanates*

Rare earth titanates of different stoichiometries are well known. Of these $RE_2Ti_2O_7$ is the most important (Minerveni *et al* 2000). Generally, $RE_2Ti_2O_7$ have pyrochlore structures (Sickafus *et al* 2000) of general formula, $A_2B_2O_7$, where 'A' and 'B' are trivalent and tetravalent metal ions, respectively which is analogous to modified cubic fluorite structure (Knop *et al* 1969; Melnik and Tsapenko 1986; Skapin *et al* 2000) except La, Pr and Nd which are having monoclinic structures. The structure and properties of the $RE_2Ti_2O_7$ (RE = La, Pr and Nd) synthesized by different methods are discussed below.

3.2 *Properties of $RE_2Ti_2O_7$ made by solid-state method*

The RE titanates obtained from the solid-state method by sintering at different temperatures exhibit thermochromic properties as given in table 1. The densities of discs also vary with sintering temperatures but generally show lower sintered densities. XRD patterns of three RE titanates indicate that the compounds formed are not phase pure, though several peaks corresponding to the monoclinic structure of the compound appeared. It leads to conclude that direct reaction of RE_2O_3 and TiO_2 by the solid state route do not yield completely phase pure $RE_2Ti_2O_7$.

3.3 *Formation of $RE_2Ti_2O_7$ by SHS method*

In the SHS methods, the combustion mixture, the nitrates and the activator, behave like conventional 'oxidants' and 'fuels' and undergo self-sustained combustion, producing ashes containing the oxide product (Varma and Lebrat 1992; Patil *et al* 2002; Bahadur *et al* 2006). During the combustion, exothermic redox reactions associated with nitrate decomposition and fuel oxidation take place. Gases such as NO_2, H_2O and CO_2 evolve favouring the forma-

tion of fine particle ashes within a few minutes. The liberation of gases favour the desegregation of the products (increases the porosity) and heat dissipation (inhibits the sintering of the products). Exothermicity of combustion is controlled by the nature of the fuel and the oxidizer to fuel ratio. The reaction paths for synthesis have been described in the literature (Borovinskaya 1992; Feng *et al* 1994; Grigoryan 1997; Moore *et al* 1997; Patil *et al* 2002).

Most of the Bragg peaks in the XRD pattern of all the compounds that are synthesized using urea as the activator and calcined at 1200°C match with the ICDD peaks of the standard monoclinic $RE_2Ti_2O_7$ but they are not completely phase pure, as shown in figure 1, the XRD pattern of $La_2Ti_2O_7$ made by SHS (urea) method.

3.4 *Advantages of $RE_2Ti_2O_7$ synthesized by SHS–ammonium acetate method*

In the case of inorganic fuel (ammonium acetate) activated SHS reactions better homogeneity of the reactants can be ensured at the beginning of the reaction, by dissolving the RE nitrates and ammonium acetate in the solvent. The added titanium dioxide powder remains homogenously dispersed in the solution, which greatly influences the SHS reaction to take place efficiently to form completely phase pure $RE_2Ti_2O_7$, compared to the product formed in the usual SHS reaction activated by the organic fuels.

In the urea activated SHS reactions the combustion leads to a flaming type of reaction (Aruna and Rajam 2004) and the flame persists for comparatively longer durations allowing the resultant nanoparticles to get sufficient time and temperature for self sintering to yield larger particles. Whereas the SHS reaction activated by ammonium acetate is much faster and does not make any persisting flames, instead at the peak of the reaction quick combustion takes place as in the burning of 'firework flower pots'. The nanoparticles formed in the reaction fly fast out of the reaction vessel and cool down very fast retaining the smaller sized particles. In addition, the urea activated SHS reactions usually produce agglomerated particles. Aruna and Rajam (2004) obtained α-Al_2O_3 of low surface area and larger sized particles in their urea activated SHS reactions due to the formation of stable polymeric intermediates that prevented heat dissipation and led to excessive flames that facilitated particle growth in the process.

An attractive feature of the modified SHS process is that while the generally used activator urea that melts at 133°C is a typical organic compound, whereas the ammonium acetate is a salt of a weak acid and weak base that possesses relatively unusual melting point of 112°C, an uncommon feature of usual inorganic salts. Ammonium acetate decomposes when heated to elevated temperatures to form acetamide as an intermediate

$$NH_4COOCH_3 \rightarrow CH_3CONH_2 + H_2O.$$

The formation of two molecular species at such mild temperatures is an uncommon phenomenon among inorganic salts.

The theoretical reaction taking place in the ammonium acetate activated SHS reaction can be represented as

$$2RE(NO_3)_3 + 2TiO_2 + CH_3COONH_4 + 1/2O_2 \rightarrow RE_2Ti_2O_7 + NH_3 + 6NO_2 + 2CO_2 + 2H_2O.$$

Properties of the nanopowders of $RE_2Ti_2O_7$, obtained in this modified SHS method, were characterized by different techniques as outlined below.

3.4a *Thermal properties*: The thermograms and DTA curves of the three RE titanates are given in figures 2(a)–(b) to 4(a)–(b). The weight loss/gain at different temperatures are presented in table 2. The data show that the weight loss occurring in the case of $La_2Ti_2O_7$ and $Nd_2Ti_2O_7$ up to a temperature of ~750°C is ~10% and only a marginal increase in weight above 750°C (However, in the case of $Pr_2Ti_2O_7$, the weight loss is 3·73% at ~450°C but it becomes 12·7% up to ~1400°C).

Similarly, the DTA data of all the SHS powder (table 3), indicate two distinct regions in the curve that correspond to exothermic and endothermic changes in the thermal behaviour of the nanopowder. The exothermic broad maxima are in the range 267–284°C and the endothermic behaviour is maximum in the range between 1043 and 1220°C. The peak heights in the exothermic region are lower and broader compared to the endothermic region.

The TG and DTA data indicate that characteristic transition takes place in the SHS material at higher temperatures of 1100–1220°C and the $RE_2Ti_2O_7$ become phase pure at around 1200°C. This has also been confirmed from the XRD patterns of the samples obtained at higher temperatures.

The compacted discs of $RE_2Ti_2O_7$ upon sintering at temperatures 1350°C, 1400°C, 1450°C, 1500°C and 1550°C exhibit a lower densification rate for the samples made by the solid state route reaching a sintered density of 82–89% of theoretical densities, whereas the SHS powders become much denser of the order of 93–95% of their theoretical densities for the compounds, $La_2Ti_2O_7$ (5·78 g/cc), $Pr_2Ti_2O_7$ (5·95 g/cc), and $Nd_2Ti_2O_7$ (6·11 g/cc). The rates of densification of the discs on sintering at high temperatures are shown in figure 5.

3.4b *XRD studies*: On examining the XRD patterns of the three RE titanates, $La_2Ti_2O_7$, $Pr_2Ti_2O_7$ and $Nd_2Ti_2O_7$ obtained in the SHS–AA reaction, in their uncalcined form as well as after calcining them at 600°, 800°, 1000° and 1200°C, it is observed that in all the cases, the resultant product of SHS reaction is amorphous or microcrystalline in nature. Upon calcining at higher temperatures

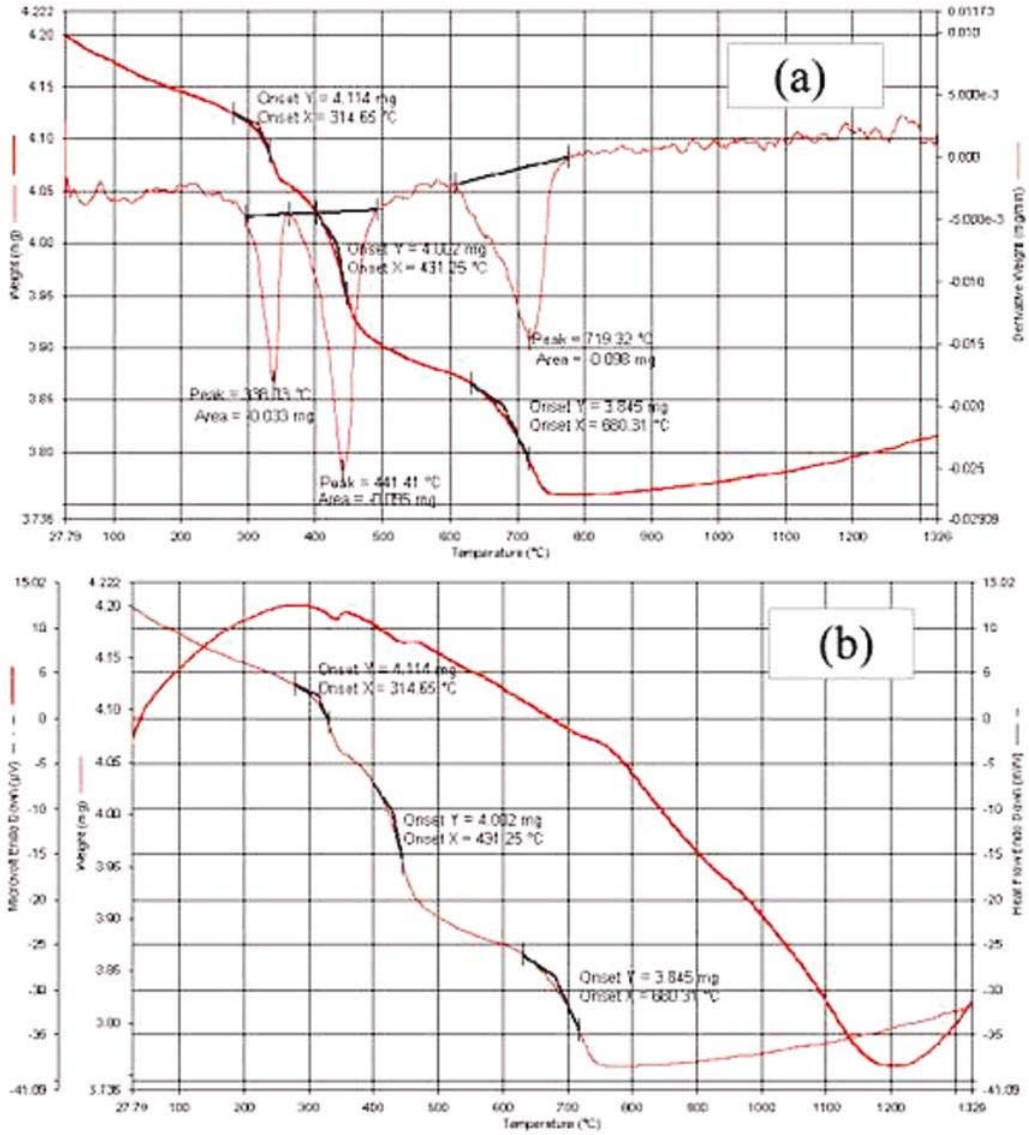

Figure 2. Thermogram (N_2) of $La_2Ti_2O_7$ synthesized by SHS-AA method: (**a**) TG–DTG and (**b**) DTA–TG.

the material improves its crystallinity and becomes phase pure monoclinic crystalline compound, as shown by their matching XRD patterns with the respective ICDD standards. As an example, the XRD patterns obtained in the case of $Nd_2Ti_2O_7$ powder, in its 'as synthesized' form and after calcining at temperatures from 600–1200°C are shown in figure 6. The synthesized SHS powder upon calcining acquires crystalline nature and transforms to pure polycrystalline material at higher temperatures. The powder calcined at 1200°C possesses 100% monoclinic structure of $Nd_2Ti_2O_7$ (ICDD: 33-492). Similar behaviour is exhibited by the nanopowders of $La_2Ti_2O_7$ and $Pr_2Ti_2O_7$, synthesized by the modified SHS method.

3.4c *FT–IR and Raman spectral studies*: As the RE titanates are compound oxides of RE_2O_3 and TiO_2, their vibrational spectra due to the inter-atomic bonding will largely be dependent on the spectral behaviour of both RE_2O_3 and TiO_2. It is well known that TiO_2 transforms from its 'anatase' phase to the 'rutile' phase on heating the material above 700°C. The TiO_2 used in the present study was separately heated to 1200°C along with the SHS powders and confirmed its formation of rutile, TiO_2, by taking its XRD.

FT–IR spectra of the monoclinic $RE_2Ti_2O_7$ calcined at 1200°C is given in figure 7. A comparison of the reported spectral data of constituent rutile, TiO_2 and the RE_2O_3 with the spectra of the RE titanates revealed that significant differences exist in the spectra of $RE_2Ti_2O_7$ in terms of the number and positions of the vibrations. Several new vibrations appeared due to various Ti–O and RE–O vibrations that changed appreciably. The FTIR spectral

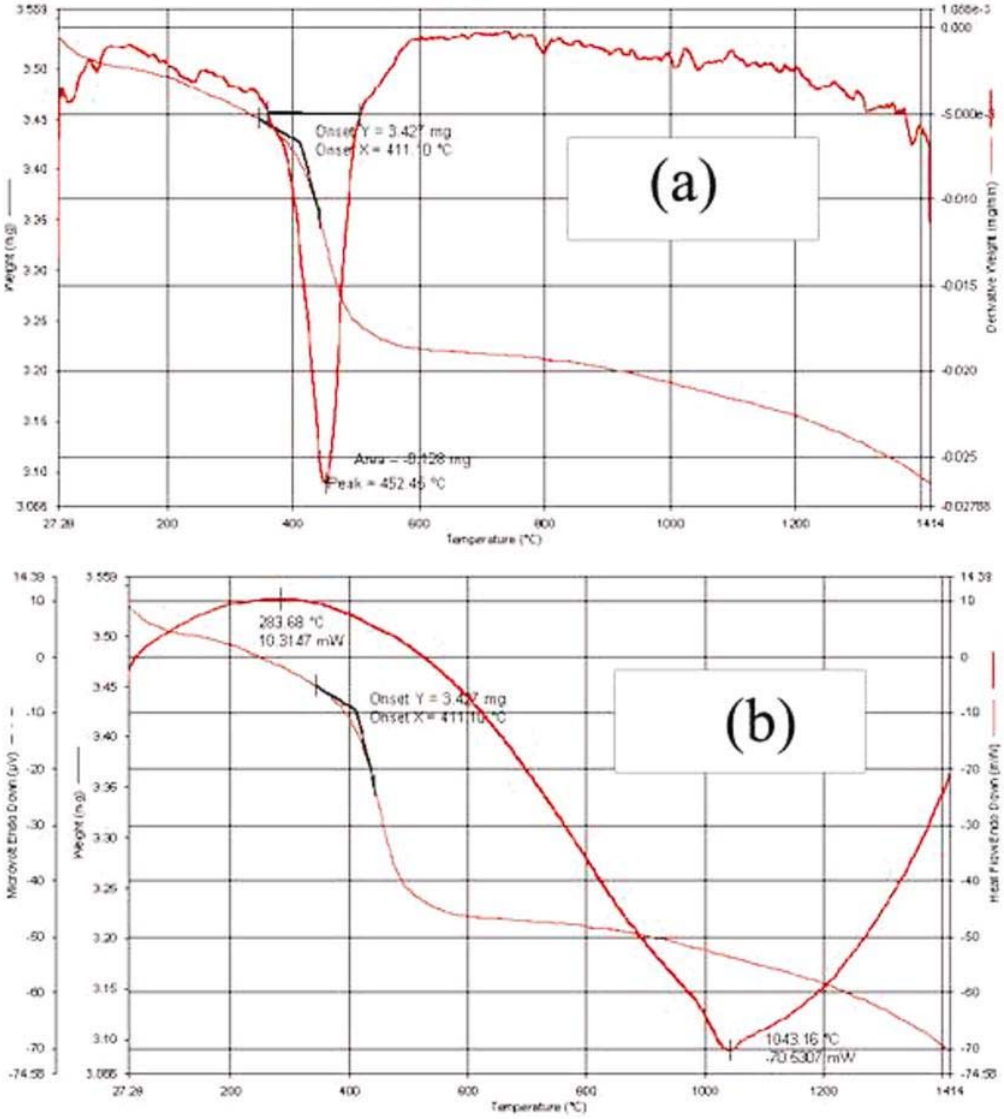

Figure 3. Thermogram (N_2) of $Pr_2Ti_2O_7$ synthesized by SHS–AA method: (**a**) TG–DTG and (**b**) DTA–TG.

bands in the frequency region of interest 400–1000 cm^{-1} is given in table 4.

Additionally, the spectral data in the region 1000–4000 cm^{-1} exhibit several weak absorptions. However, as the spectra were recorded after calcining the samples at 1200°C the presence of X–H vibrations such as O–H, N–H, C–H, etc characteristic of this region cannot be expected. Therefore, these weak absorptions may be due to overtones and combinational bands of the compounds.

The characteristic peaks (Nakomoto 1997) for rutile, TiO_2, in the Raman spectra are at positions $\mathbf{A}_{1g}$: 612 cm^{-1} (ν_S Ti–O); $\mathbf{B}_{1g}$: 143 cm^{-1}; $\mathbf{B}_{2g}$: 826 cm^{-1} and $\mathbf{E}_g$: 447 cm^{-1} (ν_{as} Ti–O). Laser Raman spectra of the three monoclinic RE titanates calcined at 1200°C were recorded in the region 400–4000 cm^{-1} and the region of interest, 400–1000 cm^{-1} is shown in figure 8. The important spectral bands and their probable assignments are given in table 5. It can be observed that all the compounds exhibited several characteristic absorptions (Nakamoto 1997), for example, the $\mathbf{A}_{1g}$ and $\mathbf{E}_g$ bands of TiO_2 remain shifted in the product, RE titanates. While the $\mathbf{A}_{1g}$ band exhibited a marginal shift, the $\mathbf{E}_g$ band shifted appreciably. Similarly the characteristic bands of the RE_2O_3 also shifted significantly in the respective $RE_2Ti_2O_7$ spectra. In addition, several new bands appeared in the spectra of $RE_2Ti_2O_7$ presumably due to the compound formation and consequent phase changes and also the effect of ionic size, RE–O bond lengths, and strengths. The extent of shift in the Raman peaks of RE titanates with reference to the rutile characteristic peaks, $\mathbf{A}_{1g}$ and $\mathbf{E}_g$, are given in table 6.

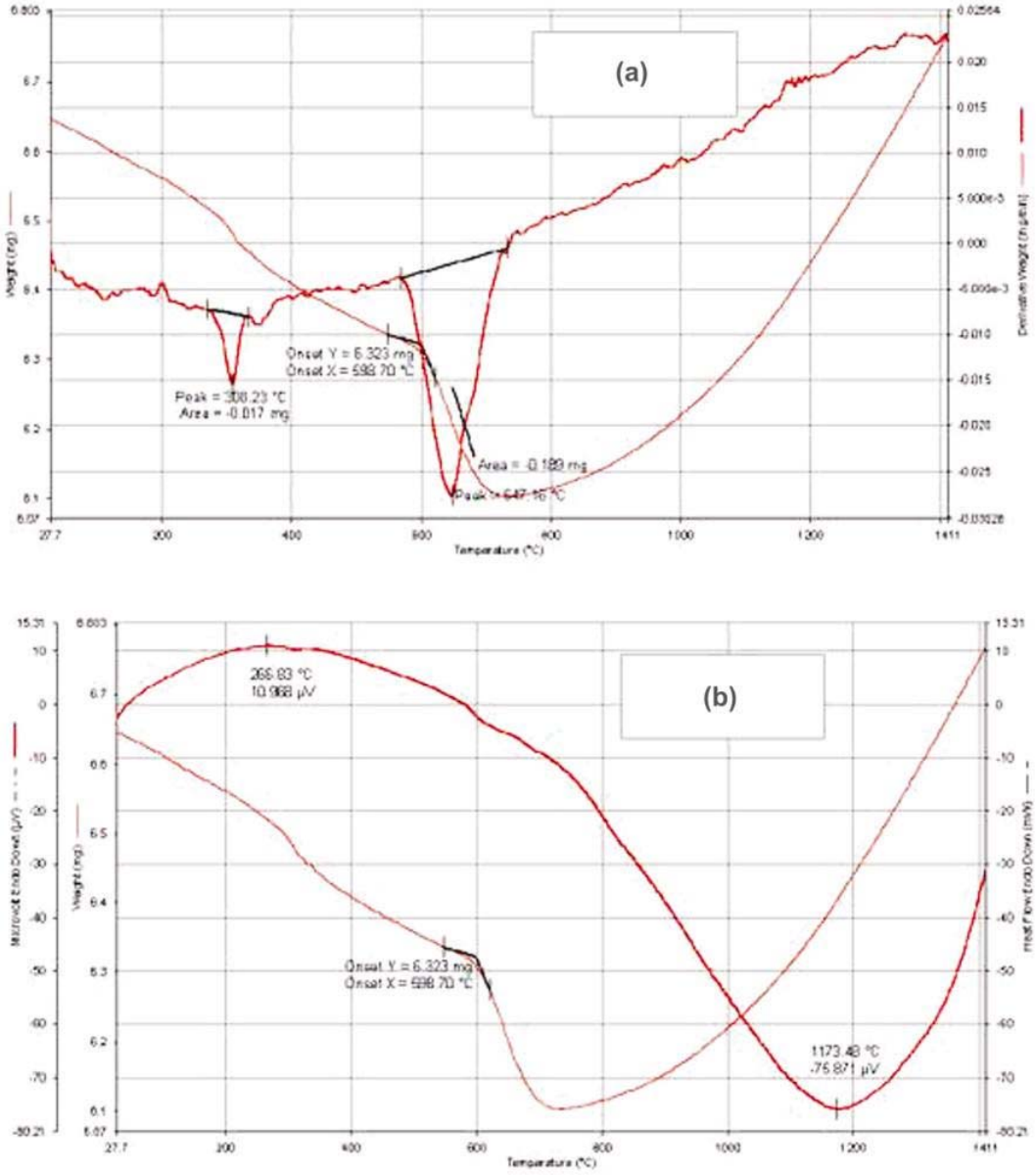

Figure 4. Thermogram (N_2) of $Nd_2Ti_2O_7$ synthesized by SHS–AA method: (**a**) TG–DTG and (**b**) DTA–TG.

Table 2. TG data of the SHS–AA powders of monoclinic $RE_2Ti_2O_7$ [RE = La, Pr, Nd].

$RE_2Ti_2O_7$	Atmosphere	Weight loss (%)	Temp. (°C)	Weight gain (%)	Temp. (°C)
$La_2Ti_2O_7$	Nitrogen	10·5	750	1·4	1326
$Pr_2Ti_2O_7$	Oxygen	12·7	1414	–	–
$Nd_2Ti_2O_7$	Nitrogen	8·1	760	10·0	1411

3.4d *BET surface area measurements*: Results of the surface area measurements of the synthesized nanopowders of La and Nd titanates and calculation of their particle sizes show that the powders have an average particle size (APS) in the 61–91 nanometer range. $Pr_2Ti_2O_7$ powders were soft agglomerates which possessed an APS of 311 nm and the surface area and APS values are given in table 7. After measuring the values of relative pressure in nitrogen atmosphere, the BET plots were made for $1/[W((P_O/P) - 1)]$ against relative pressure, P/P_O and the surface area and particle size of the three monoclinic RE titanates were calculated.

Table 3. DTA data of SHS powders of monoclinic $RE_2Ti_2O_7$ [RE = La, Pr, Nd].

$RE_2Ti_2O_7$ (atmosphere)	Temp. maxima		Peak values of reaction			
			Exothermic		Endothermic	
	Exothermic (°C)	Endothermic (°C)	Value (μV)	Temp. (°C)	Value (μV)	Temp. (°C)
$La_2Ti_2O_7$ (N_2)	675	1326	12·600	275·00	–38·50	1220·0
$Pr_2Ti_2O_7$ (O_2)	555	1414	10·315	283·68	–70·53	1043·2
$Nd_2Ti_2O_7$ (N_2)	580	1411	10·968	266·83	–75·87	1173·0

Table 4. Characteristic FT–IR bands of monoclinic $RE_2Ti_2O_7$ in the range of 400–1000 cm^{-1}.

$La_2Ti_2O_7$	$Pr_2Ti_2O_7$	$Nd_2Ti_2O_7$	Probable assignments
804 m	814 w		A_{2u}-LO of TiO_2 (811)
			E_u-LO of TiO_2 (806)
760 m	766 w	720 mbr	
	625 m		
561 sbr	571 m	525 mbr	
488 s	471 m	469 s	E_u-LO of TiO_2 (458)
467 m	446 m		RE-O(B)
442 s			
420 m			

w = weak; m = medium; s = strong; br = broad.

Table 5. Important Raman spectral bands of the monoclinic $RE_2Ti_2O_7$.

$La_2Ti_2O_7$	$Pr_2Ti_2O_7$	$Nd_2Ti_2O_7$	Probable assignments
884 w	816 s	824 m	B_{2g} TiO_2 (826)
804 m	796 s	794 m	
729 w		684 wbr	
654 w			
615 m	608 w	614 m	A_{1g} TiO_2 (612)
567 w	580 w	574 m	RE-O(A)
529 w	552 w		
	472 m		
456 m	464 m	440 m	Eg TiO_2 (447)
412 m			
351 m	360 s	370 s	RE-O(D)
		347 s	
248 s	282 vvs	277 vs	RE-O(G)
163 vvs	172 vs	172 vvs	RE-O
124 m		124 s	RE-O(I)
61 mbr			

3.4e *SEM microstructures*: The SHS powders are generally very fluffy in nature with sponge like interconnected porous network, which can easily be smashed to particles of very fine size of the order of < 100 nm. The SEM microstructures of the monoclinic RE titanates are shown in figure 9. The SEM photographs showed very fine sizes of the order of nanometer ranges of the powders. The $La_2Ti_2O_7$ and $Nd_2Ti_2O_7$ powders appear to be free in nature with fewer interconnections of the particles compared to $Pr_2Ti_2O_7$ powder, which is not relatively free but remain loosely interconnected in a porous network that would lead to apparently lesser surface area and large particle size. This observation is in agreement with BET

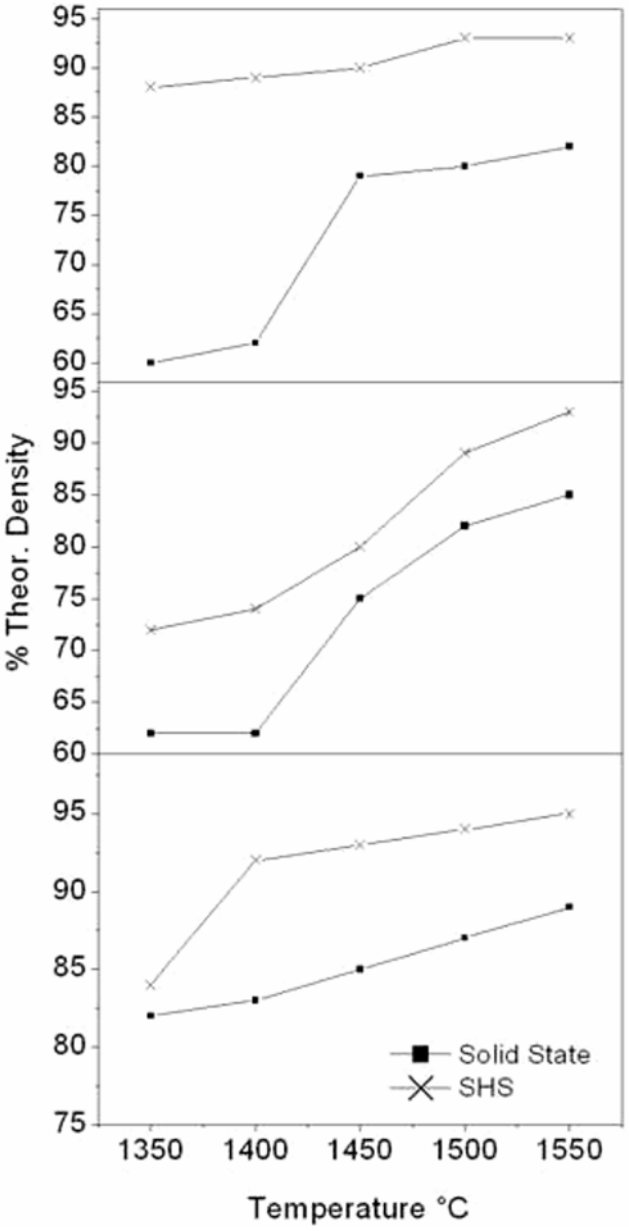

Figure 5. Densification of $RE_2Ti_2O_7$ samples on sintering at high temperatures.

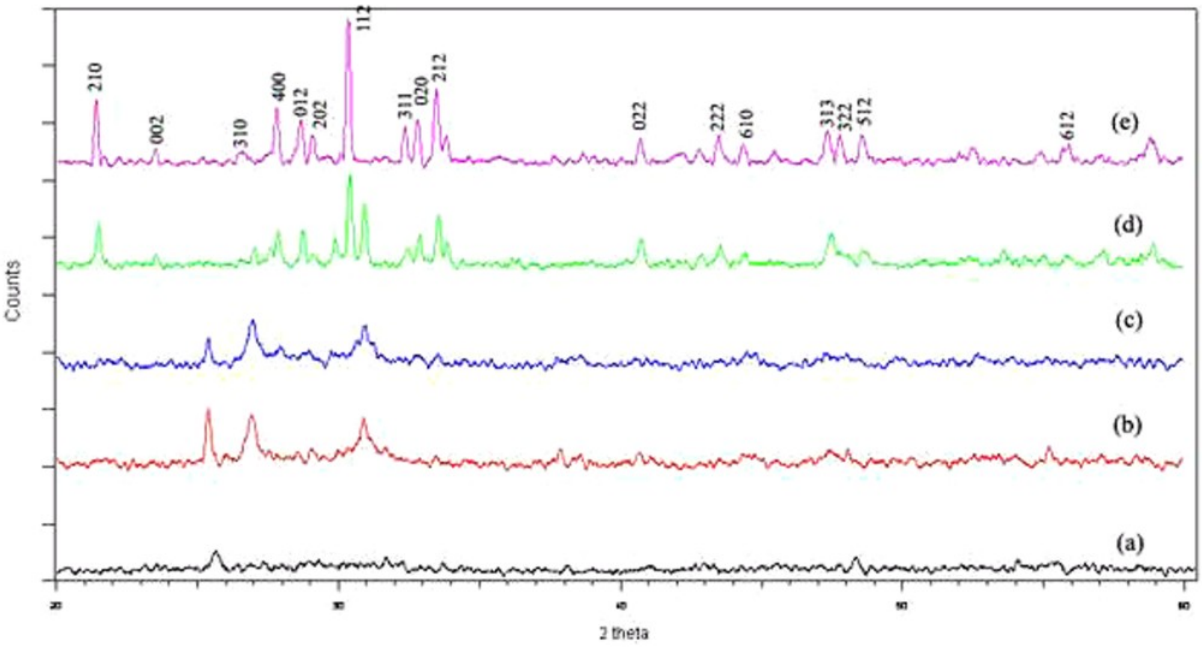

Figure 6. XRD patterns of $Nd_2Ti_2O_7$: (a) SHS powder, before calcination, (b) calcined at 600°C, (c) 800°C, (d) 1000°C and (e) 1200°C (Match ICDD 33-0942 Monocl. $Nd_2Ti_2O_7$).

Table 6. Percentage shift in the Raman peaks of $RE_2Ti_2O_7$ compared to rutile peaks A_{1g} and E_g.

	Wave number (cm^{-1}) and % shift			
	Equivalent to A_{1g} (612)		Equivalent to E_g (448)	
$RE_2Ti_2O_7$	Value	% Shift	Value	% Shift
$La_2Ti_2O_7$	615·40	0·56	456·19	1·83
$Pr_2Ti_2O_7$	608·00	–0·65	464·00	3·57
$Nd_2Ti_2O_7$	613·18	0·19	439·72	–1·85

Table 7. BET surface area and APS of monoclinic $RE_2Ti_2O_7$ synthesized by SHS method.

$RE_2Ti_2O_7$ (RE =)	Density (g/cc)	Surface area (m^2/g)	APS (nm)
La	5·78	11·4	91
Pr	5·95	3·24	311
Nd	6·11	16·01	61

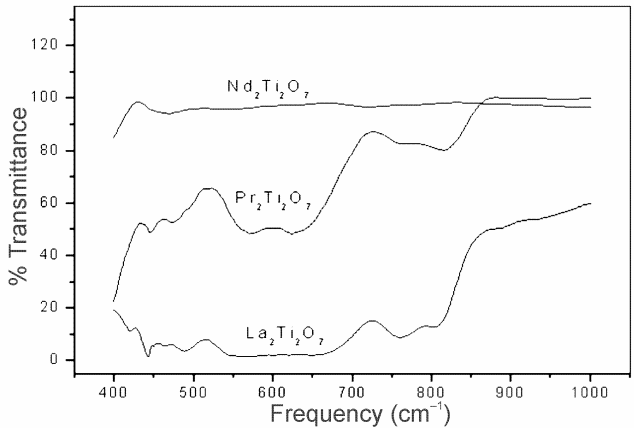

Figure 7. FTIR of monoclinic $RE_2Ti_2O_7$ synthesized by SHS method and calcined at 1200°C (400–1000 cm^{-1}).

surface area measurements. The powder samples of $La_2Ti_2O_7$ and $Nd_2Ti_2O_7$ have lesser average particle sizes and more surface area but $Pr_2Ti_2O_7$ is found to have lesser surface area and hence larger particle size.

The SEM microstructures of the sintered monoclinic RE titanates exhibit a well-sintered physical appearance for the broken cross-sectional structure for the discs. The grains are so smoothly interconnected with almost zero porosity and appear to be well sintered. The SEM microstructures of the cross sectional surfaces of the sintered discs are given in figure 10.

3.5 *Dielectric properties*

For the sintered (at 1550°C) samples made by the SHS method and solid state method the changes in permittivity (ε_r) with frequency (100 Hz to 10 MHz) are shown in figure 11 and the variation in dissipation factor with frequency in figure 12. It is evident from figure 12 that the dissipation factor approaches stable values in the higher frequency range above 10 kHz and it remains highly stable in the MHz ranges. The change in permittivity (ε_r) with temperature (figure 13) exhibited a positive temperature coefficient of capacitance (TCC) with increasing temperature. To make it suitable for temperature stable

dielectrics, it is to be mixed with materials of negative TCC to form solid solutions.

It is observed that, in general the dissipation factor values are high for solid-state samples, for example, it is 0·506 (at 10 KHz) to 0·181 (at 100 KHz). The corresponding values for SHS samples are 0·016 (at 10 KHz) and 0·004 (at 100 KHz). At higher frequencies, 1 MHz and above, both solid-state and SHS samples have dissipation factor values in the range 0·002–0·006 only. Thus the RE titanates synthesized by SHS method exhibit good dielectric behaviour with high permittivity values that are stable in the higher frequency ranges.

Usually titanates are employed as dielectric material for the production of capacitors and microwave dielectrics (Shulman *et al* 1996; Alvarez-Fregoso 1997). While the alkaline earth titanates, $MgTiO_3$, $CaTiO_3$, $SrTiO_3$ and $BaTiO_3$ possess very high dielectric constant values with a sharp peak at their ferroelectric Curie temperatures (Yanagida *et al* 1996; Rama Mohan *et al* 1998), the RE titanates are found to have low dielectric constant values, which remain almost constant at different temperatures. This peculiar property makes the RE titanates and their doped compositions to be attractive candidates for microwave applications as resonators etc (Jung *et al* 1996; Sebastian *et al* 2001; Paschoal *et al* 2003).

4. Conclusions

Phase pure monoclinic rare earth titanates, $RE_2Ti_2O_7$ (RE = La, Pr, Nd), can be synthesized in their nanometer size by the modified SHS method using ammonium acetate as the activator of SHS reaction. Dielectric properties of

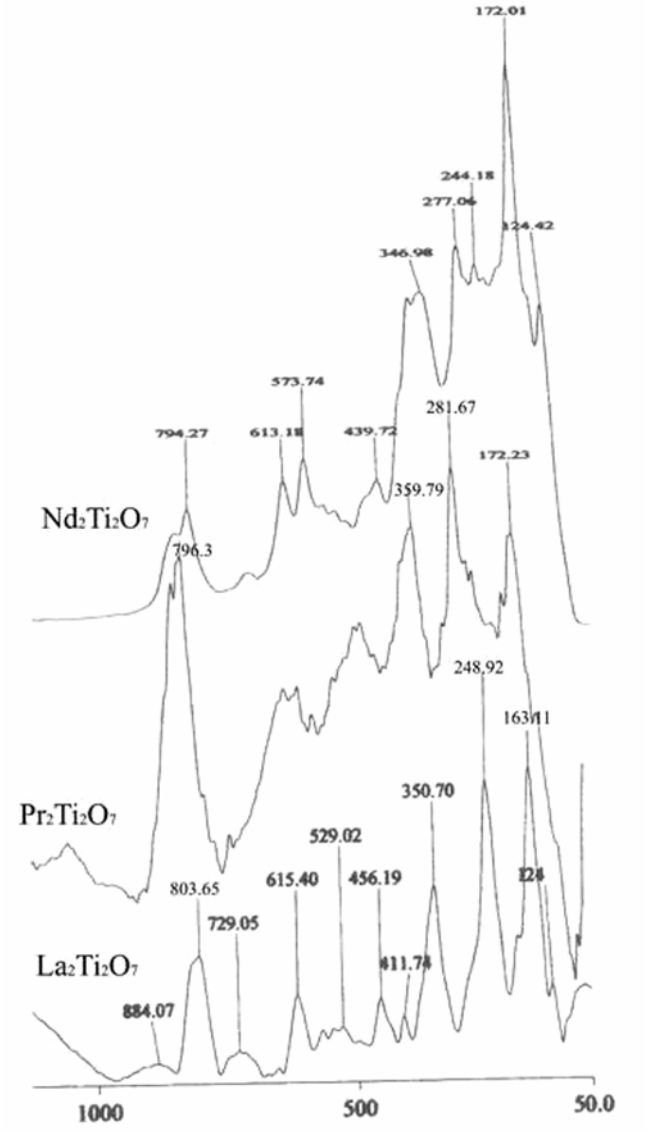

Figure 8. Raman spectra of the SHS powder of monoclinic $RE_2Ti_2O_7$ calcined at 1200°C.

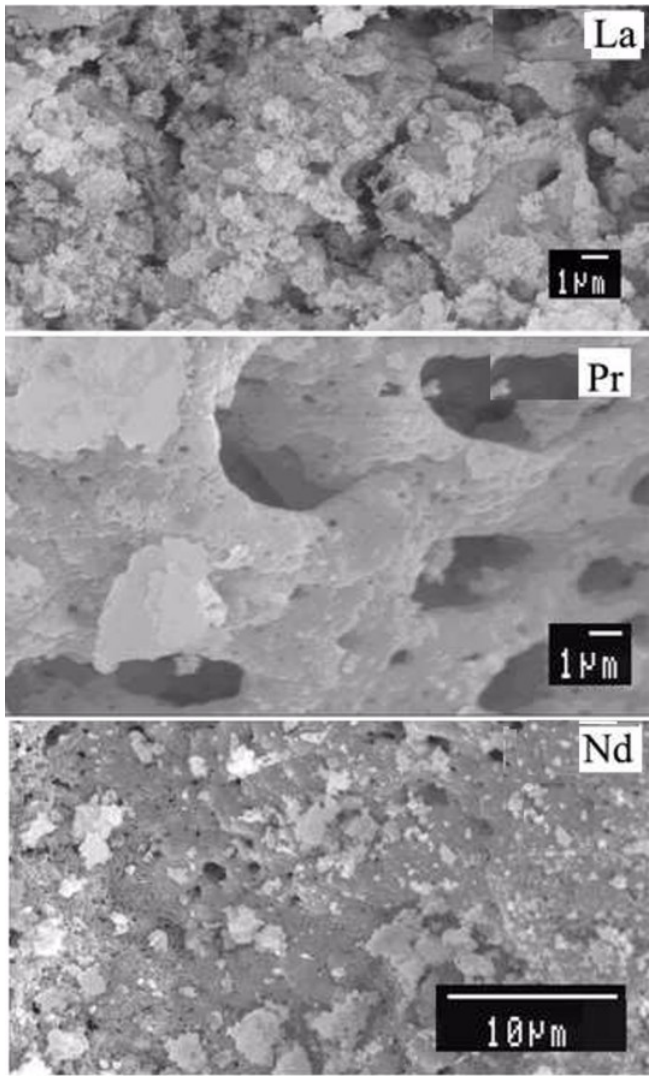

Figure 9. SEM microstructure of SHS powders of monoclinic $RE_2Ti_2O_7$.

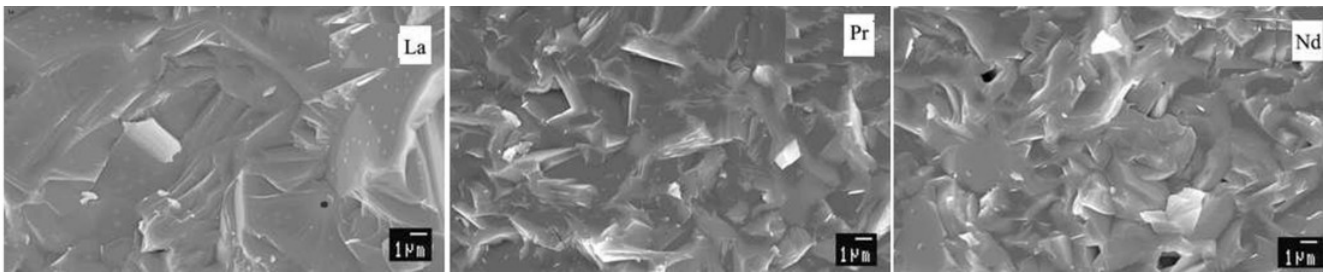

Figure 10. SEM of the cross section of sintered discs of monoclinic $RE_2Ti_2O_7$ made from SHS powders.

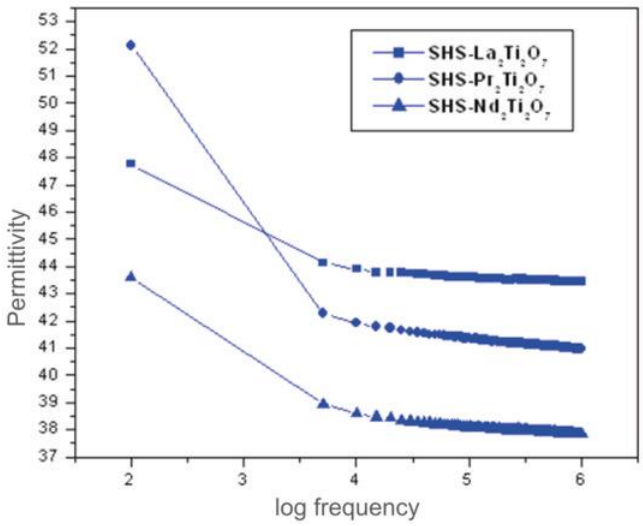

Figure 11. Changes in permittivity with frequency of monoclinic $RE_2Ti_2O_7$ sintered at 1550°C.

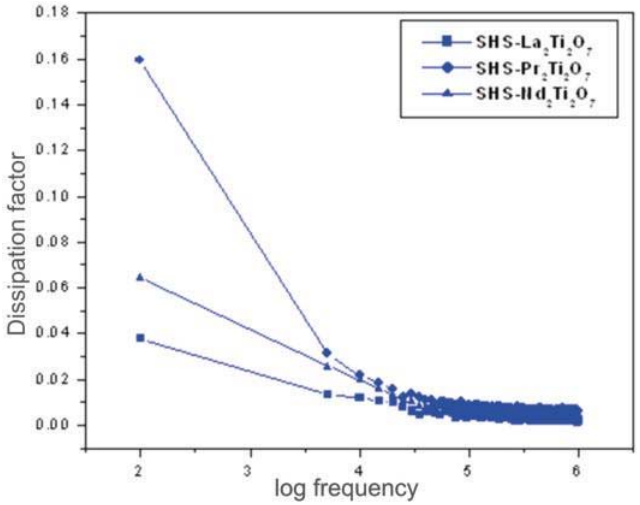

Figure 12. Changes in dissipation factor with frequency of monoclinic $RE_2Ti_2O_7$ sintered at 1550°C.

components made from the SHS powders are superior to those synthesized by the solid-state method and found to exhibit high stability in the rated characteristics at high

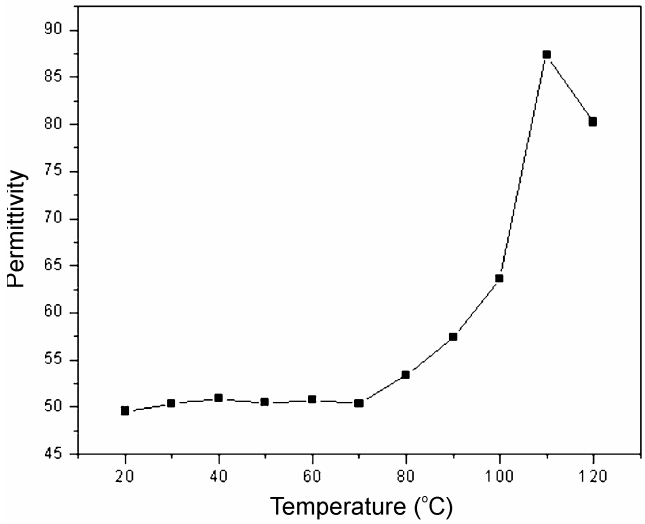

Figure 13. Changes in permittivity with temperature for the monoclinic, $La_2Ti_2O_7$ synthesized by SHS method.

frequency ranges (1 KHz–10 MHz). It has low dissipation of 0·002–0·004. Thermal studies and XRD confirm formation of phase pure crystalline compounds at around 1000°C. Thus the modified SHS method offers a cost effective and energy efficient process for the synthesis of high quality $RE_2Ti_2O_7$ material suitable for high frequency dielectric applications.

References

Alvarez-Fregoso Octavio 1997 *J. Appl. Phys.* **81** 1387
Aruna S T and Rajam K S 2004 *Mater. Res. Bull.* **39** 157
Bahadur D, Rajakumar S and Ankit Kumar 2006 *J. Chem. Sci.* **118** 15
Borovinskaya I P 1992 *Pure & Appl. Chem.* **64** 919
Buchanan R C 1993 *Ceramic materials for electronics* (New York: Marcel Dekker Inc.)
Chaput F, Boilot J P and Beauger A 1990 *J. Am. Ceram. Soc.* **73** 942
Feng H J, Hunter K R and Moore J J 1994 *J. Mater. Synth. Process* **2** 71
Grigorev Y M and Merzhanov A G 1992 *Int. J. SHS* **1** 600
Grigoryan E H 1997 *Int. J. SHS* **6** 307

Hwang Chyi-Ching, Wu Tsung-Yung, Wan Jun and Tsai Jih-Sheng 2004 *Mater. Sci. & Engg.* **B111** 49
Jung H J *et al* 1996 US Patent 5569632
Katayama S, Yoshinaga I, Yamada N and Nagai T 1996 *J. Am. Ceram. Soc.* **79** 2059
Kestigian Michael and Ward Roland 1955 *J. Am. Ceram. Soc.* **77** 6199
Kimura M *et al* 1972 *Jpn J. Appl. Phys.* **11** 904
Knop Osvald, Brisse Francois and Castelliz Lotte 1969 *Canadian J. Chem.* **47** 971
Liu Xiao Qiang and Chen Xiang Ming 2005 *J. Am. Ceram. Soc.* **88** 456
Matkowsky B J, Aldushin A P, Shkadinsky K G and Shkadinskaya G V 1997 *Int. J. SHS* **6** 345
Melnik N N and Tsapenko L M 1986 *Inorg. Mater.* **22** 575
Minervini L R, Grimes W and Sickafus K E 2000 *J. Am. Ceram. Soc.* **83** 1873
Moore J J, Kunrath A O, Torres R, Reimanis I, Mustoe G, Upadhya K and Levashov E A 1997 *Int. J. SHS* **6** 277
Nadkarni U 1991 *Fine ceramic powders–British Ceramic Proceedings* (eds) R Freer and J L Woodhead **47** 81
Nakamoto Kazuo 1997 *IR and Raman spectra of inorganic and coordination compounds* (New York: John Wiley & Sons)
Paschoal C W A, Moreira R L, Fantini C and Sebastian M T 2003 *J. Eur. Ceram. Soc.* **23** 2661
Patil K C, Aruna S T and Mimani T 2002 *Curr. Op. Solid State Mater. Sci.* **6** 507
Rama Mohan T R, Sood D D, Vaidya V N and Ram Prasad 1998 *Fine ceramics – synthesis, properties and applications* (India: Indian Ceramic Society Pub.)
Reed J S 1989 *Introduction to the principles of ceramic processing* (New York: John Wiley)
Sebastian M T, Soloman S and Ratheesh R 2001 *J. Am. Ceram. Soc.* **84** 1487
Scheunmann K and Muller H K 1975 *J. Inorg. Nucl. Chem.* **37** 1879
Shulman H S, Testorf M, Damjanovic D and Setter N 1996 *J. Am. Ceram. Soc.* **79** 3124
Sickafus K E *et al* 2000 *Science* **289** 748
Skapin S D, Kolar D and Suvorov D 2000 *J. Eur. Ceram. Soc.* **20** 1179
Takeda H *et al* 2003 *Jap. J. Appl. Phys.* **42** 6081
Varma A and Lebrat J P 1992 *Chem. Eng. Sci.* **47** 2179
Xiong S B *et al* 1996 *Appl. Phys. Lett.* **69** 191
Yanagida Hiroaki *et al* 1996 *The chemistry of ceramics* (USA: John Wiley & Sons)